



OpenAIR@RGU

The Open Access Institutional Repository at Robert Gordon University

<http://openair.rgu.ac.uk>

This is an author produced version of a paper published in

JBIS: Journal of the British Interplanetary Society (ISSN 0007-084X)

This version may not include final proof corrections and does not include published layout or pagination.

Citation Details

Citation for the version of the work held in 'OpenAIR@RGU':

MACLEOD, C., 2013. Innovative approaches to fuel-air mixing and combustion in airbreathing hypersonic engines. Available from *OpenAIR@RGU*. [online]. Available from: <http://openair.rgu.ac.uk>

Citation for the publisher's version:

MACLEOD, C., 2013. Innovative approaches to fuel-air mixing and combustion in airbreathing hypersonic engines. *JBIS: Journal of the British Interplanetary Society*, 66 (5/6), pp. 178-189.

Copyright

Items in 'OpenAIR@RGU', Robert Gordon University Open Access Institutional Repository, are protected by copyright and intellectual property law. If you believe that any material held in 'OpenAIR@RGU' infringes copyright, please contact openair-help@rgu.ac.uk with details. The item will be removed from the repository while the claim is investigated.

INNOVATIVE APPROACHES TO FUEL-AIR MIXING AND COMBUSTION IN AIRBREATHING HYPERSONIC ENGINES

CHRISTOPHER MacLEOD

School of Engineering, The Robert Gordon University, Aberdeen, Scotland, AB10 1FR, UK.

This paper describes some innovative methods for achieving enhanced fuel-air mixing and combustion in Scramjet-like spaceplane engines. A multimodal approach to the problem is discussed; this involves using several concurrent methods of forced mixing. The paper concentrates on Electromagnetic Activation (EMA) and Electrostatic Attraction as suitable techniques for this purpose - although several other potential methods are also discussed. Previously published empirical data is used to draw conclusions about the likely effectiveness of the system and possible engine topologies are outlined.

Keywords: Scramjet, mixing, EMA, controlled compression mixing, flow driven fuel system

1. INTRODUCTION

It is now around sixty years since the first serious attempts to produce a Scramjet engine. The progress made during the intervening time has been intermittent. Although new techniques like Computational Fluid Dynamics (CFD) mean that more is known about some of the detailed questions of aerodynamics, the current designs are little different to those suggested two generations ago. In recent years, programmes like HyShot, HyCause and the X-43A have again added to our knowledge but, despite optimistic claims from vested interests, extended flight under Scramjet power remains almost just as elusive as in the past.

There are several reasons why this is the case, some are due to the difficulty of designing the inlet and exhaust topologies for the extended flight envelope and similar mechanical-engineering concerns. However, although such issues are demanding, they have proved soluble in other aerospace applications and the most challenging aspect of Scramjet technology lies in fuel mixing and combustion.

In the high-drag and high-temperature regime where Scramjets operate, it is difficult to add further kinetic energy to an already excited flow-stream. This means that the engine is operating in a finely balanced region in terms of its thrust and drag and good conversion of the fuel's chemical energy into usable flow-energy is essential. However, at hypersonic speeds, air passes through the engine in around a millisecond, meaning that the fuel must mix with the air, burn and release its energy in a few tens of microseconds [1]. To achieve maximum extraction of energy, the fuel must be mixed stoichiometrically with air, at the molecular level, during this time. These operations should be performed in a way which does not disrupt the flow enough to cause an increase in drag. The resulting mixture has also to be burnt without the aid of the flameholding structures used at lower speeds - as projections into the duct would cause form-drag. Such considerations make it obvious why the technology is on the edge of practicality [2].

This paper builds on previous work [3, 4], published in *JBIS*, to suggest some engine topologies which might be used as a basis for experimentation or simulation into overcoming

the mixing problem. For reasons discussed in the paragraphs below, these are not final design solutions, but are meant as a basis for discussion on Scramjet topologies and related issues.

In the work presented here, it is suggested that the answer to the mixing problem might lie in a multimodal system – that is, a system in which several different and complementary techniques are employed in order to achieve the mixing goal. In particular, the paper outlines how previous work on Electro-Magnetic Activation (EMA) and Electrostatic Attraction could be used to enhance and control the mixing and ignition process. Other potential methods that might be used in a multimodal system, including a new “flow-driven” concept, are also discussed.

The fuel-air mixing system in a scramjet engine is difficult to simulate accurately using techniques like CFD. Some of the physical phenomena present are hard to study - because of the speeds and temperatures involved, and are therefore rather poorly understood. Others, because they represent elements of both non-continuum (free molecular) and continuum (Navier-Stokes) flow or complex systems of interacting flows, are not readily amenable to standard modelling equations or simulation techniques. This is particularly true of the methods outlined in this paper, because they themselves are innovative in their approach and use unusual topologies and techniques to address the mixing problem.

Although modelling and simulation are difficult for the reasons outlined above, quite a number of authors have published their observations on applicable systems and these can be used to build useful conclusions. Therefore, the approach taken here is to base some of the discussion on previously published empirical and experimental results. It is for this reason, as already mentioned, that the suggestions presented are not final design solutions, but are meant to stimulate ideas for discussion. However, it is hoped that they can form the basis of future experiments or simulations to establish their credibility.

The paper deals with the dynamics of the fuel-air mixing

and combustion system and not with the aerodynamic design of the ducts or surfaces of the engine. This is because there are already many published analyses of these [2, 5]. Where it is necessary to state aerodynamic or flow parameters, figures from a well known design by Billig [6], discussed in Anderson [7], will be used. This design and its associated flow parameters are typical of the available examples and have been used in many previously published papers.

The discussion starts with a description of traditional mixing in scram systems and then goes onto discuss EMA assisted mixing, electrostatically assisted mixing, other multimodal approaches and finally some possible engine topologies.

2. THE CONVENTIONAL VIEW OF MIXING

In order to understand issues with the mixing process and how it may be improved, it is first necessary to understand its dynamics in more detail.

There are three simplified cases which illustrate the basic mechanisms of unforced mixing. The first is zero-shear mixing, which assumes inviscid flow. In this circumstance, the fuel and air mix by simple diffusion only - there are no shear forces or macroscopic mixing due to turbulent flow.

Although this type of mixing is not practical due to its slowness, it is nevertheless an important case to understand. This is because, as mentioned in the previous section, there needs to be stoichiometric mixing at the molecular level for good energy extraction - and only diffusion (simple or forced) can supply this. So, no-matter how much the fuel is enfolded in the air by turbulence or other macroscopic mechanisms, the two components still need to diffuse into each other. Simple diffusion is controlled by Fick's Law, the form of which can be found in any textbook on the subject [8]. The special case of diffusion of two gases is covered in reference [9]. The topology usually considered is shown in Fig. 1.

The mixing layer, of fully diffused gas, thickness δ , grows down-stream [2] and has the approximate width:

$$\delta \approx 8\sqrt{\frac{Dx}{u}} \tag{1}$$

Where D is the molecular diffusivity for air and the fuel, x is the distance along the axis of the duct from the point of contact and u is the average of the speed of the air and fuel. The air and fuel will be completely mixed when δ is equal to the width of the duct b ($= b_1 + b_2$ in Fig. 1). The length along x required to fulfil this condition (denoted L) is:

$$L = \frac{ub^2}{16D} \tag{2}$$

Working out some practical figures for required mixing lengths and fuel velocities shows that L/b is of the order of 1500. Such long engines are not practical because of the associated skin-friction losses [5].

In the second mixing case, viscous laminar interaction is allowed - this is called the Laminar Shear Case [10], here:

$$\delta = 8\sqrt{\frac{\nu x}{u}} \tag{3}$$

Where ν is the kinetic viscosity (μ/ρ). Perhaps surprisingly, this produces no great improvement over the zero-shear case - because lateral movement is still by molecular processes.

In the final case, by increasing the velocity difference between the two streams or by other similar means, Kelvin-Helmholtz Instability may be induced and hence turbulent mixing. Here mixing is much more efficient because the generated vortexes entrain the fuel and air components and allow for contact at small scales. It is difficult to derive theoretical models for this, but several empirical surveys do exist. One useful and oft-cited treatment of turbulent mixing [11] showed that:

$$\delta = C\left(\frac{1-r}{1+r}\right)x \tag{4}$$

Where C is a constant reported to be between 0.25 and 0.45 in various experiments, and r is the ratio of the velocities of fuel and air.

Inserting some typical figures into this equation shows that turbulent mixing is much more efficient at producing mixing in a fairly short length of duct. However, the induction of instabilities in the flow is a macroscopic process - therefore slow and, in any case, diffusion is still necessary across the entrained fluid boundaries to achieve the molecular mixing necessary for efficient combustion. These factors mean that the achievement of a true stoichiometric mixture, in the time allowable, is still very difficult.

To induce turbulent mixing of the type described above, normal injection solutions (that is, fuel is injected "normally" or perpendicularly to the airflow) have been introduced as shown in Fig. 2.

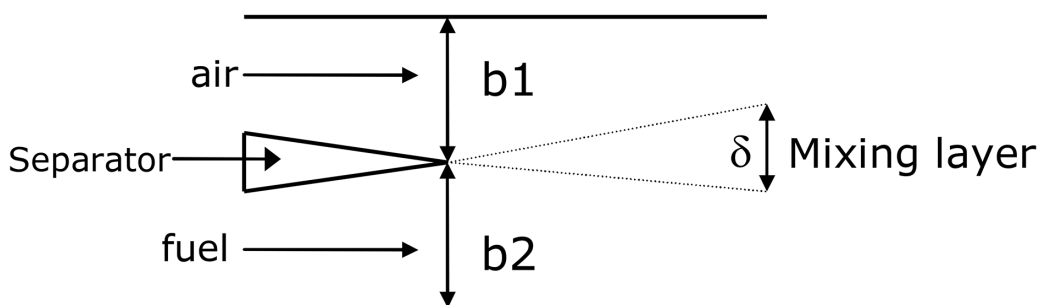


Fig. 1 Topology for zero-shear mixing.



Fig. 2 Normal and ramp injection.

One obvious problem with this is that such injection necessarily causes disruption to the flow and therefore strong shock interactions. These result in further drag - particularly if the boundary-layer is disrupted, as it inevitably will be. Further, this will inhibit mixing for the reasons discussed in the next section. Unfortunate inlet to combustor interactions may also upset the duct pressure balance and cause unstart [1]. Hence, even without considering compressibility issues, there are two conflicting requirements on the system, firstly good mixing but secondly minimum disruption to the flow.

The scale of the problem presented above can be seen by using some typical figures available for practical flow-speeds, fuels and engine lengths; for example, using Billig’s engine design [6]. In this case, given that the maximum diffusion coefficient of hydrogen into air is around $2.6 \text{ cm}^2 \text{ s}^{-1}$ [8] (just below its auto-ignition temperature with air, at a typical Scramjet combustor pressure [6]), then the air and hydrogen must be turbulently mixed or entrained over the entire volume to a contact dimension of between a few millimetres and a centimetre if diffusion is going to act within the time available for complete mixing at high Mach [9]. Although this is a very difficult engineering task, it is not impossible to envisage that a viable Scramjet can be achieved. However, the results from actual scramjet tests do not show the predicted power output, and therefore something is wrong with the model. The most likely reason for this is discussed in the next section.

3. COMPRESSIBILITY AND MIXING

Results in a number of published papers demonstrate why the simple theoretical treatment of mixing presented in the last section needs revision. These results revolve around issues involving the relative speed (and therefore compressibility) of the two mixing flows (the air and fuel). They show quite clearly that, if the flows are relatively supersonic (as they would be in many practical mixing scenarios, like normal injection), the mixing layer is much smaller than if they are subsonic relative to each other.

Some of the important papers in this field are by Papamoschou

and Roshko who, in their best known paper [12], present an extensive set of experiments and a theoretical framework. Azim and Islam [13] also carry out similar experimental work and again find that (to quote their abstract): “The mixing layer growth was found to decrease with increasing velocity ratio.” Earlier work which also supports these findings includes Birch and Eggers [14] and Brown and Roshko [15], among others.

Although there is much debate about a theoretical framework to support such results, they certainly seem to be a product of compressibility phenomena. Consider, for example, a subsonic flow and one which is relatively supersonic; where these two flows meet, a shockwave forms. Although the shockwave is thin, it still represents a high density discontinuity between the flows. This region is maintained only by the energy flowing into the system, as this is required in order for the flow molecules to maintain their positions in equilibrium. The forces on the individual molecules have the form shown in Fig. 3 [16].

To the molecules on the lower energy side of the shock, the shock region is effectively a barrier to penetration (and therefore diffusion) - as to move into it would mean moving, against a steep energy gradient, into the area labelled “A” in Fig. 3. Even before shockwaves form, a region of increased compression exists which can have a similar effect. To quantify the amount of compression at the boundary between the flows, many authors define a relative speed for the flow components (essentially shifting the frame of reference from the laboratory to that of the free flow). This is often termed the convective Mach number M_c . A common definition for two flows is:

$$M_c = \frac{u_1 - u_2}{a_1 + a_2} \tag{5}$$

Where u_1 and u_2 are the speeds of the flows under consideration and a_1 and a_2 are the speed of sound in these flows.

In a theoretical and review paper [17] Slessor and his co-

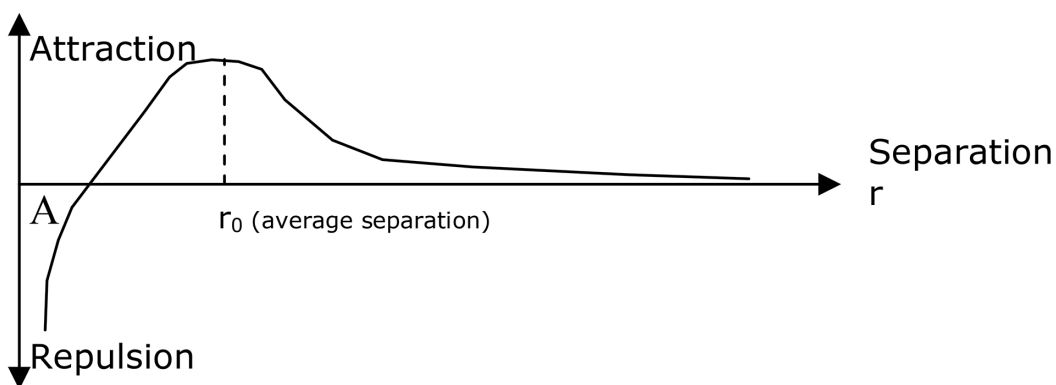


Fig. 3 Forces on flow molecules.

authors present a survey and consolidation of the results from ten previous experimental papers published between 1966 and 1998. Figure 4 shows a graph plotted from this data. In this graph, the spatial rate of increase of the shear layer thickness is labelled δ' and the growth rate of the layer at $M_c = 0$ is labelled δ'_0 (sometimes called the incompressible growth rate):

$$\delta' = \left. \frac{d\delta}{dx} \right|_{\delta=f(M_c)} \quad \text{and} \quad \delta'_0 = \left. \frac{d\delta}{dx} \right|_{M_c=0} \quad (6)$$

So the term δ'/δ'_0 is the rate of change of the mixing layer, normalised to the incompressible case.

It can be seen from the graph that the amount of mixing decreases rapidly with increasing M_c . It also appears to tend asymptotically to a value of around $\delta'/\delta'_0 \approx 0.2$, particularly for $M_c > 1$.

There are several issues with this interpretation of the data, however. Firstly, most of these experiments measure the size of the shear or turbulent layer rather than the mixing layer per say. This means that the figures should not be taken as measure of the extent of an even approximately stoichiometric mixture – this would be much more difficult to establish and almost impossible to measure at realistic speeds. A second issue is that, although Slessor *et al* have correlated the data from a number of experiments, there are still only around forty data points available. The high cost and specialised equipment needed for such investigations mean that this will be the case for the foreseeable future. Finally, not all the available data is consistent. Several sets show distributions which indicate that maximum rate growth is not at $M_c = 0$. For example, the data measured by Hall *et al* [18], is typical of the shape of these curves, as shown in Fig. 5 (on the same scale as Fig. 4). Such data usually shows a peak in the region $0.2 < M_c < 0.8$ and this may be related to the triggering of turbulent mixing in such setups.

Slessor and his co-workers acknowledge such results and point-out they tend to occur at large density or velocity ratios (which is important, since one or both these conditions usually apply in the case of fuel-air mixing). They propose a new measure of compressibility (labelled Π_c), to integrate more of the outlying data points into an overall expression:

$$\Pi_c = \frac{\sqrt{\gamma_{(\max)} - 1}}{a_{\max}} (u_1 - u_2) \quad (7)$$

Where $\gamma_{(\max)}$ is the maximum specific heat ratio between the flows under consideration (there may be more than two) and similarly a_{\max} is the maximum speed of sound of the components. However, as the authors themselves point out, not all the data fits even this formulation.

As discussed in the paragraphs above, there are problems with the available experimental data. These may be summarised as: lack of agreement on the theoretical basis of the effects observed, a general lack of experimental data and data sets which do not sit well with proposed “best fit” lines and curves. However, despite this, it is clear that, to a first approximation, mixing efficiency generally decreases with increasing compression (velocity ratio) between flow components. It is therefore essential that any experimental mixing system provides the ability to supply the fuel so that performance can be maximised. This is a technically difficult task. The next

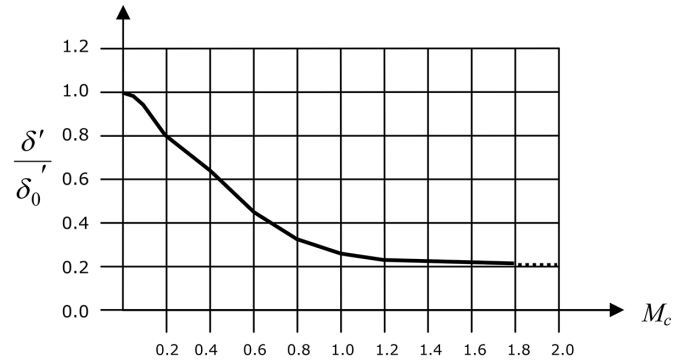


Fig. 4 Graph generated from data presented in Slessor *et al* [17].

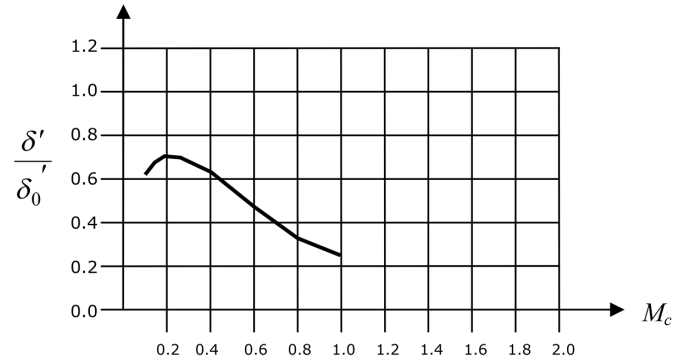


Fig. 5 Graph generated from data presented in Hall *et al* [18].

section discusses how it might be achieved using a technique previously published in *JBIS – Electromagnetic Activation or EMA*.

4. EMA ENHANCED MIXING

As discussed in the previous section, there is considerable debate over some of the physical mechanisms involved in mixing (and some of the more subtle aspects involved were also neglected in the description above for simplicity). However, the data clearly shows that the difference between optimal and worst-case laminar mixing efficiency is up to 500%. It is therefore imperative that the system supplying fuel to the airflow is able to provide it in a way which maximises the mixing effectiveness. In a real system, this means that (primarily) the speed must be controlled - but also (secondarily) the temperature, density and interaction angle. The EMA system discussed below is potentially capable of providing this flexibility (both in terms of experimental and final systems).

The principle idea behind EMA is that a fluid (either in a flow or at rest) is heated by Electromagnetic Radiation emitted into the fluid and absorbed by it. This radiation directly activates the fluid at the molecular level, increasing its internal energy by coupling to its rotational, translational, vibrational or electronic energy modes. A detailed theoretical discussion of this, together with derivations of the fundamental equations, is contained in previous papers [3, 4].

There are several ways in which EMA can be used in propulsion concepts. These include: Firstly, heating the airflow directly using millimetre-wave frequencies or ultraviolet light. This possibility was discussed extensively in the original papers [3, 4]. Secondly, adding a substance with high absorbance to the working fluid. This heats-up efficiently and transfers energy to the main flow (the components of pure air normally have a

rather low absorbance). Thirdly, heating the flow so much that some of its components disassociate and high-energy chemical reactions can occur, which add further energy (for example, in air, reactions involving the nitrogen components). Finally, the case being considered here: using EMA to accelerate or activate the fuel (or flow) in a more conventional scramjet type system with the aim of increasing its mixing efficiency.

The original papers mainly discussed adding heat to flow through open ducts; however, exactly the same principle can be applied to closed ducts like chambered de-Laval nozzles, as shown in Fig. 6.

As shown in the original EMA papers, the path-length x required to absorb a particular proportion of the radiation is given by:

$$x = \frac{\ln\left(1 - \frac{\varpi}{100}\right)}{-(\sigma n)} \tag{8}$$

Where ϖ is the percentage of radiation to be absorbed; for example, if this figure was 99%, then x would be the distance required to absorb 99% of the radiation power. The symbol σ is the Absorption Cross Section of the species involved, usually specified in cm^2 (in which case, x is in cm) and n is the number density of the species in particles per cm^3 .

The radiation propagates in the duct by wall or mirror reflection in a similar way to propagation along a waveguide. The required mirror length D of a parallel sided structure, like that shown in the figure, is given by:

$$D = x \sin \theta \tag{9}$$

Where θ is the launch angle measured from a normal to the duct wall. The temperature rise of the fluid, in the radiation field, for a given mass flow-rate and absorbed power is:

$$\Delta T = \frac{\xi}{\dot{m}C} \tag{10}$$

Where C is the Specific Heat Capacity of the gas and ξ is the absorbed radiation power. The mass flow-rate may be calculated from $A\dot{v}$ (where A is the cross-sectional area of the chamber). Knowing these figures, it is then possible to calculate the exist velocity of a nozzle with choked flow:

$$v_e = \sqrt{\frac{2T_c R \gamma}{w(\gamma - 1)} \left[1 - \left(\frac{p_e}{p_c}\right)^{\frac{\gamma-1}{\gamma}} \right]} \tag{11}$$

Where T_c is the chamber temperature, w is the molecular weight of the working fluid, R is the gas constant and p_e and p_c are the pressures in the chamber and at the exit of the nozzle.

One important aspect of using radiation to heat the flow like this is its controllability and flexibility. The power applied to the fluid can be regulated electronically and although the example above illustrates a topology similar to a conventional rocket motor, this need not be the case. Because the heating effect may be applied at any point in the system, the shape of the nozzle or duct can be carefully controlled to provide a flow of any density, speed and temperature. EMA therefore has the capability of producing a much more flexible result than other alternatives like high pressure guns or simple electric heating.

In general, there are three options for EMA activated fuels. The first is simply to activate the fuel directly. The main way of doing this is to use a fuel molecule with a dipole moment - these can generally be activated in the microwave or millimetre parts of the spectrum [19, 20]; alternatively the vibrational modes of the molecule can be activated in the infrared [21]. Using micro or millimetre waves may be preferable, because of the efficiency and flexibility of the available sources (discussed in detail in [4]). Many hydrocarbons and other molecules can be activated like this [22] and The American Institute of Standards and Technology maintains on-line records of microwave absorption bands in the Hydrocarbon Spectral Database at its Physical Measurement Laboratory. Unfortunately however, many important simpler substances, like H_2 and CH_4 , have no intrinsic rotational moment by virtue of their molecular symmetry.

The second option is to create or induce a dipole in an unpolarised fuel molecule. The ways of doing this are to either apply an external electric field (which acts to skew the shell electronic field and produce a polarised result); or alternatively, the electronic configuration of the molecule can be changed (usually by ionising it). Adding energy in this way has been explored in hydrazine thrusters [23].

The final option is to mix a high absorption substance in with the fuel - so that this heats up and transfers its energy to the non-absorbing fuel. As a simple example, consider water.

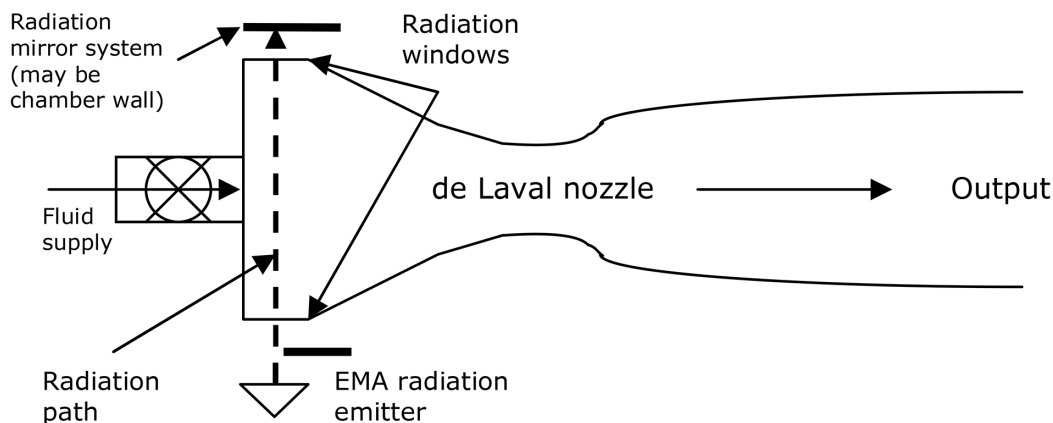


Fig. 6 Rocket-like EMA system.

This absorbs at several microwave and millimetre wave frequencies – for example 22 GHz, 183 GHz and 325 GHz [24]. In a atmosphere of H₂ or a light hydrocarbon at Standard Temperature and Pressure (STP) where 1% of the molecules are water, half of the energy at 183 GHz will be absorbed in an 8 metre path-length and 92% in a 67 metre path-length; at 325 GHz almost all the energy is absorbed within a couple of centimetres.

Table 1 shows the power required to accelerate the fuel to the same speed as the airflow, using such an EMA system, in a Scram-like topology, based on Billig’s figures for inlet conditions [6, 7]. The combustion output power is 100 MW (similar to a large turbojet) and the EMA system is assumed to be 40% efficient. The mixture ratio for H₂ is 1:4 by weight (as normally used in practical rocketry), rather than the stoichiometric 1:8; similarly for Kerosene, it is assumed to be 1:3.

From Table 1 it can be seen that the EMA system consumes between around 0.80% of the total power output (for H₂ at Mach 5) to nearly 60% (for kerosene at Mach 25). This illustrates the main issue with accelerating the fuel – the system is directing kinetic energy into the fuel electromagnetically, rather than thermally as in a rocket motor and so the overall efficiency will always be lower than in a topology where the fuel does not have to be speeded up. In a practical system, as much waste heat-energy as possible from the rocket cowl would be recaptured using heat exchangers to help power the EMA system.

The discussion above also assumes that the fuel feed is in-line with airflow. This is unlikely in reality as best mixing will probably occur at some other angle. Figure 7 shows the multiplying factor of the fuel velocity when subject to different angles of incidence with airflow (from 1 at 0° as just discussed to ∞ at 90°).

Using a system like this also raises several other possibilities. One of these is to chemically “engineer” fuels to have exactly the right properties. For example, a fuel with a useful dipole moment could be synthesised, as could one which flew apart during activation to produce lighter products, or a folded fuel with a reactive centre which only unfurled as it rotated (or conversely, two products which only became active when they react). Another interesting possibility is that, because the fuel and air stream are moving at similar speeds, the fuel could be added to the airflow with “swirl” (a rotational component) to aid mixing. This is usually ineffective in more conventional systems due to losses associated with the shock interactions between the fuel and airstream.

Overall, the system might have a topology similar to that shown in Fig. 8. This is not to scale, but is meant to illustrate a possible layout of the various components. The combustion and exhaust structure is illustrated here as an aerospike so that they operate in a rocket-like mode and avoid the need for

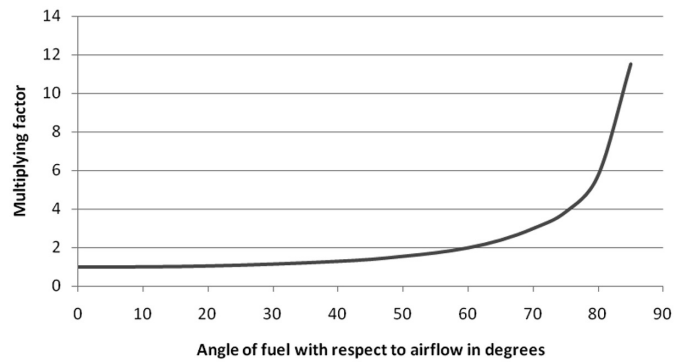


Fig. 7 Effect of angle of fuel injection with respect to airflow.

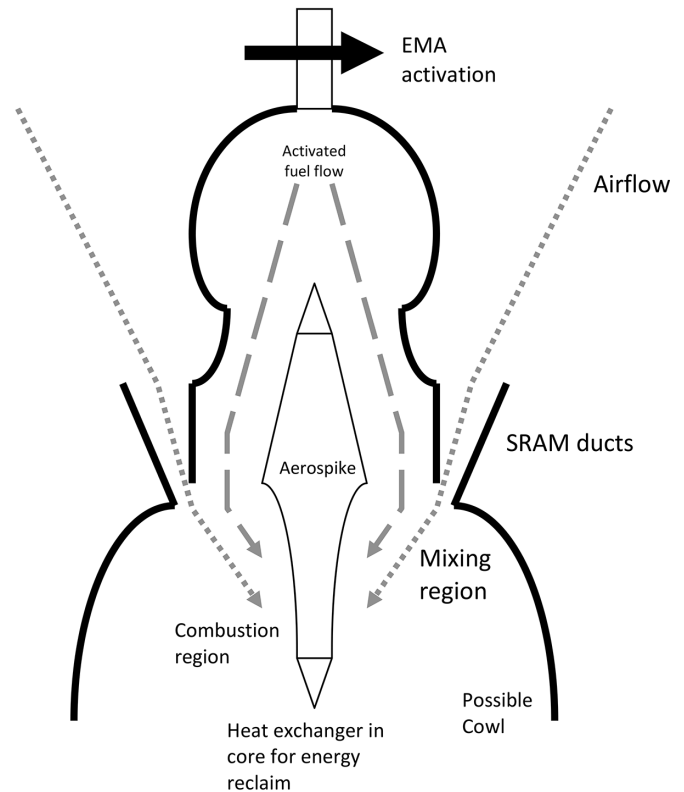


Fig. 8 Possible configuration topology.

flameholding structures (the EMA system is also capable of providing ignition energy if required). Such a structure also facilitates changeover between cycles in a combined-cycle system (for example, air breathing and conventional rocket).

5. ENHANCED MIXING USING FLOW-DRIVEN FUEL

The EMA system illustrated in the last section is not the only way to accelerate the fuel to match airflow speeds; electrical heating systems like arcjets, resistojets and others offer alternatives [25]. These are not reviewed here, as they are well

TABLE 1: Power Consumed by EMA System at Various Speeds.

Free stream Mach number	5	10	15	20	25
Speed at mixer inlet (ms ⁻¹)	561	1089	1650	2211	2739
EMA power into H ₂ fuel system (MW)	0.785	2.65	6.77	12.0	18.75
EMA power into Kerosene (RP-1) System (MW)	2.351	8.24	20.28	36.0	56.26

covered in the literature - this discussion will instead focus on methods which have not been explored in detail elsewhere. One such idea draws the acceleration energy for the fuel more directly from the momentum (and therefore output power) of the engine - rather than an intermediate electrical system like EMA. Consider first a quantity of fuel at rest in a duct, as shown in Fig. 9a. If this is impinged on by a supersonic flow as shown in Fig. 9b, a shockwave passes through it and it almost instantly accelerates to essentially the same speed as the impinging flow, this is mediated by the viscosity of the gas and is normally accompanied by an increase in temperature, Fig. 9c.

This situation is extensively studied in shock tubes [26]. The air coming in from the left is known as the driver (or “pusher” in the discussion below) and the stationary fuel, the driven. Although the gases mix slightly at their interface [27], they remain essentially separate, providing that their density ratio is low enough. Since the driven gas is initially stationary, there will be a strong interaction between it and the high-mach driver and so, to a first approximation, strong shock limits may be applied. In this case, the following relationships give the pressure, density and temperature ratios of the two gases:

$$\frac{p_2}{p_1} = \frac{2\gamma M}{\gamma + 1} \quad \frac{\rho_2}{\rho_1} = \frac{\gamma + 1}{\gamma - 1} \quad \frac{T_2}{T_1} = \frac{(2\gamma^2 + \gamma)M}{(\gamma + 1)^2} \quad (12)$$

Where the subscript 1 applies to the incoming gas and 2 applies to the stationary one. M is the mach number of the incoming flow (assuming, of course, as in the discussion above, a reference frame where the fuel is stationary).

To understand how this can be applied in a practical system, consider the following topology, shown in Fig. 10. The layout is similar to that for the EMA system shown in Fig. 8. The scram

ducts, through which the main airflow passes, are permanently open. The fuel pusher ducts are opened and closed by a rotary valve, which may be attached to a rotating noise-cone. The cycle starts as shown Fig. 9a, with the injection of fuel when the valve is shut. When the valve opens it exposes the fuel to supersonic flow from the free-stream as shown in Fig. 9b. This accelerates the fuel as shown in Fig. 9c. It then exits into the main air flow at a similar speed. The cycle then repeats.

By having several pusher ducts which open, one at a time (or alternatively, symmetrically on opposite sides), a “Gatling-gun” type system could be set up, with some ducts closed and loading while others are open. In this way, fuel may be injected in a reasonably continuous cycle. A variation of this is to interlace the fuel-pusher and air ducts, so as to create a “sandwich” of air and fuel streams - this configuration is shown in Fig. 11.

This topology has some advantages over the EMA system outlined in the previous section. As stated earlier, the power to accelerate the fuel is derived mostly from the forward momentum of the engine – and therefore more directly from the combustion of the fuel (and so practical efficiency should be higher). Although power is still needed to turn the rotary valve and redirect the flow, this is equal to power-density difference between the two flow states and is much less than the power directly supplied to the EMA system. The nose-valve opening can be profiled to minimise the transient disruption to the flow as it moves.

There are also some disadvantages with this method. Firstly, it obviously introduces moving parts into the system and needs careful mechanical design. Secondly, the system is less controllable – there might be a particular problem with temperature of the fuel (unlike the EMA system, the fuel is in contact with an oxidiser as it is accelerating) – this makes the

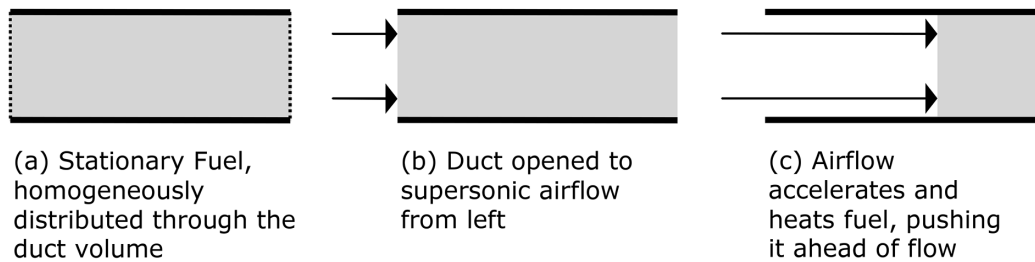


Fig. 9 A stationary gas impinged on by a supersonic flow.

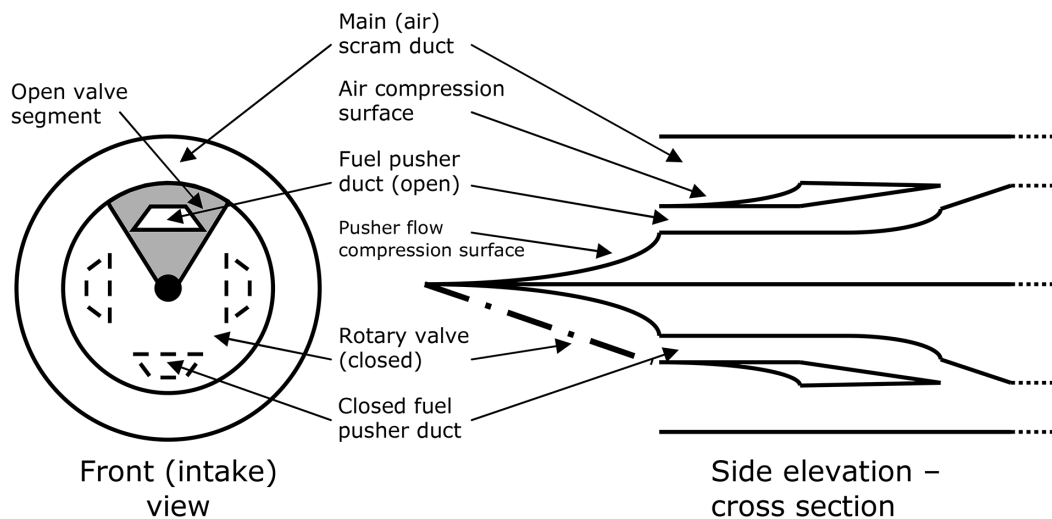


Fig. 10 Fuel pusher system using rotary valves.

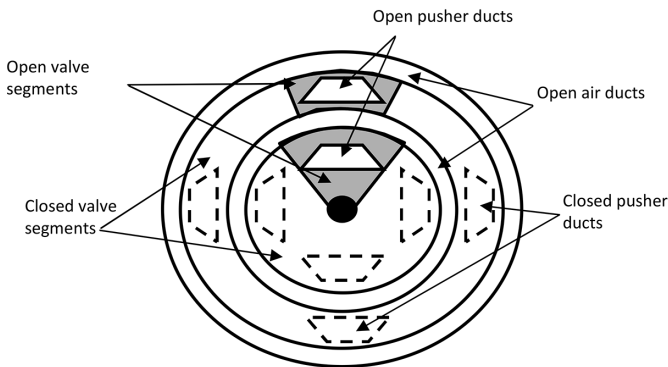


Fig. 11 Interlaced fuel and air topology.

design of the pusher-duct aerodynamics critical as their topology can control the temperature (temperature problems may also be overcome perhaps using pre-cooling of the fuel or duct, insulating pads or a buffer gas). Finally, the system is pulsed, which may cause vibration, stress or combustion problems.

There are many variations on the theme and possible combinations with the EMA method already described. For example, a system like this could be used to power the EMA device or provide mixing of the airstream with a radiation-absorbing gas. Alternatively, more than one gas could be used – for example: one pushing on the other and acting as an inert buffer, part of a two component fuel or a fuel premixed with a radiation-absorbing gas. Likewise, it may be possible to control the density ratio of the fuel and air so that the air mixes with, rather than drives, the fuel. However, this would probably require the fuel to be in a low density state (so that the flow was non-continuum and did not form a normal shock at the boundary).

6. ELECTROSTATIC ENHANCEMENT

One of the theses of this paper is that several different methods of forced or enhanced mixing may be used together to achieve good molecular penetration of the fuel into the air-stream. These approaches may be expected to be much more effective in the absence of the compressibility effects (and hence fluid-boundary shocks) discussed in the preceding sections. This approach was termed multimodal in the introduction. One potentially important method, which may be used with techniques already discussed, is electrostatically enhanced mixing. In this case, the fuel (or air) is charged and attracted into the air (or fuel) stream by a static charge as shown in Fig. 13.

In such a circumstances there are several forces acting on the fuel ions as shown in Fig. 13.

The electrostatic force is due to the field generated by the plate. Its magnitude is given by:

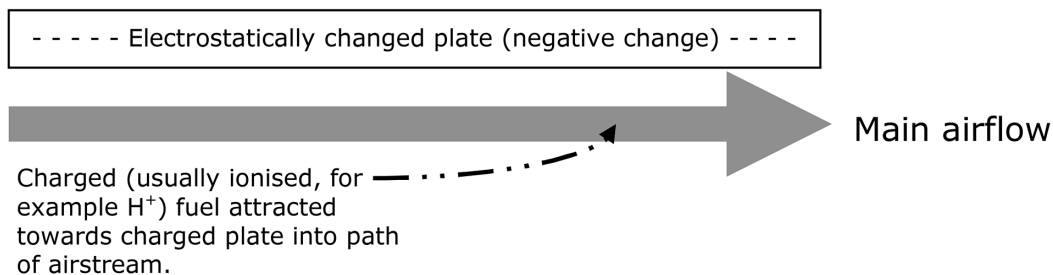


Fig. 12 The principle behind electrostatically enhanced mixing.

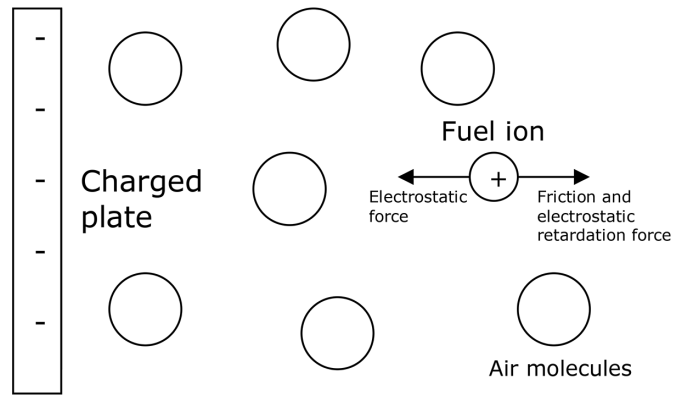


Fig. 13 Forces acting on a fuel ion.

$$F = qE \tag{13}$$

Where q is the ionic charge and E is the electric field magnitude. Expressions for E in various topologies are given in any relevant textbook [28]. The magnitude of the friction and retardation forces are complex, however the speed v of the ion can be simply expressed in terms of its mobility μ in air:

$$v = \mu E \tag{14}$$

The mobility varies with fluid parameters like density, temperature and composition and is also variable and non-linear at extremes of field intensity and viscosity. Many researchers have made measurements of ion mobility in air – from early workers [29, 30] to more recent attempts [31]. These values vary somewhat, but at the conditions of interest here, the minimum quoted values for small positive ions are around $1.15 \times 10^{-4} \text{ m}^2\text{V}^{-1}\text{s}^{-1}$ (often quoted as $1.15 \text{ cm}^2\text{V}^{-1}\text{s}^{-1}$), a figure which is inversely proportional to air density [32]. Small negative ions typically have higher values. Using the available figures conservatively and assuming an electrical field of $0.5 \times 10^6 \text{ Vm}^{-1}$ (a sixth of the typical air breakdown field at STP $\approx 3 \times 10^6 \text{ Vm}^{-1}$), the depth of the mixing layer, assuming electrostatic forcing only, may be evaluated as shown in Table 2.

These figures mean that electrostatic enhancement should approximately double (being conservative), the penetration of the fuel into the airflow, and perhaps increase it (being optimistic) by up to a factor of ten.

It might also be possible to increase the effect by using both air and fuel ions as shown in Fig. 14a. Other variations are also possible, for example modulating the charge on the plate spatially or temporally, Fig. 14b (a strong magnetic field would also achieve a similar effect). By moving the field generating potential to different positions along the plate, the ions could be directed into different positions of the airstream, so affording control which may be varied over

TABLE 2: Penetration of Ionised Fuel into Air Stream Under Electrostatic Forcing Using Billig's Figures.

Free stream Mach number	5	10	15	20	25
Speed at mixer inlet (ms^{-1})	561	1089	1650	2211	2739
Time taken for main flow to move 0.5m (μs)	891	459	303	226	183
Penetration of fuel in to stream in 0.5m stream movement (cm)	4.5	2.3	1.5	1.1	0.9

Figures are for small positive ions (very conservatively) $\mu = 1 \times 10^{-4} m^2V^{-1}s^{-1}$ in a field of $0.5 \times 10^6 Vm^{-1}$ medium is air at inlet to mixer in Billig's design [6, 7].

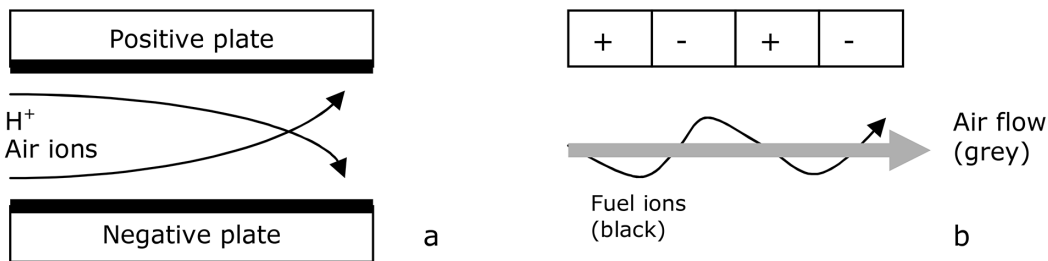


Fig. 14 Other field topologies.

the flight envelope. Fuel ions might also be accelerated along the engine axis as an alternative to the other methods already discussed.

In reality, since the fuel is initially confined, it should be much easier to ionise than the airflow [33]; indeed the EMA system itself could be designed to achieve this.

This system might be integrated into the previously discussed engine topology as shown in Fig. 15 (the central spike would be charged if the airflow were ionised).

7. OTHER APPROACHES

As well as the techniques discussed above, there are several other methods which could potentially help to enhance the mixing process. These are more speculative and so are only reviewed qualitatively.

The first such method is to use a diverter to force fuel into the airstream, Fig. 16. If the fuel is travelling at a similar speed to the airstream as previously discussed, the force from the diverter, which may include a shockwave boundary, should help to drive the fuel into the air.

Possible ways of implementing such a system are to use a rocket to generate the diverter stream – which, in turn, could be an EMA system, as already discussed or, alternatively, to use explosive diversion. This option is made more realistic by the recent development of new explosive materials which disintegrate producing fast molecular products [34, 35]. These could also be introduced into the fuel in pellet form.

Another potentially useful technique is to utilise Gas Dynamic Laser (GDL) effects. Because the composition of the fuel mixture can be controlled tightly in both the EMA and pusher topologies outlined above, inert gasses (particularly carbon dioxide) can be added to the fuel or generated in exhaust products. This allows a suitably shaped duct to generate a lasing effect [36] due to the thermally invoked population inversion. Such an effect could be used for a variety of purposes within the

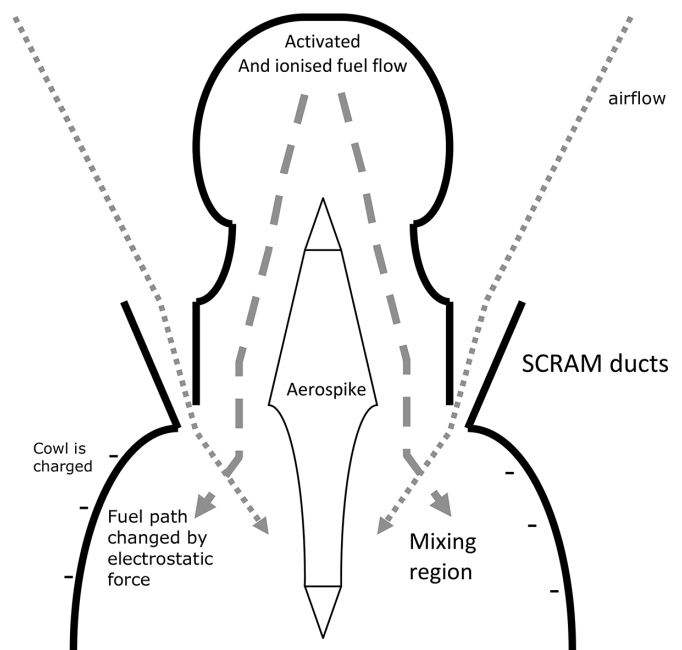


Fig. 15 Engine with added electrostatic forcing.

system. These include the extraction of energy from the stream in the form of (typically infrared) light. This energy may be used to power other subsystems, to remove heat from the flow (to produce a cooling effect) or to transfer it from one part of the flow to another (for example, from an inner duct to a bypass system). In turn, this might be used to aid mixing by increasing the internal energy in a controlled fashion or provide ignition.

8. PERFORMANCE PREDICTIONS AND ENGINE DESIGN VARIANTS

As explained in the sections above, there are several reasons why making predictions about mixing in hypersonic engines is difficult, and both the theoretical estimates and the measured results are subject to large uncertainties. This is particularly true of fuel injection and mixing techniques which produce complex flow patterns. One example of this is normal and steep-ramp

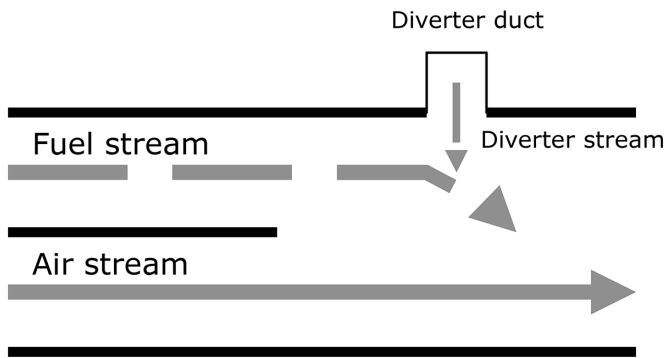


Fig. 16 Diverter operation.

injection (Fig. 2). In these cases, there is an initial normal or almost normal shock at the point where the fuel is released; this is a situation similar to the air-fuel interface at the inlet of the “pusher” topology discussed in section 5. Further downstream, the shock becomes oblique and eventually disappears as the fuel speeds up. Finally, the flow mixes turbulently in a similar way to that predicted by equation 4 (but, due to the shockwaves, well downstream of the initial contact region).

Although such issues make the mixing situation, using the techniques discussed in the previous sections, difficult to predict accurately, it is still possible to estimate performance. These predictions are based on the work presented in the earlier part of the paper and also on other published measurements and modelling of injection and mixing systems [37, 38], they are presented in Fig 17. Figure 17a shows predicted normalised mixing layer expansion enhancement. Here the symbols δ' and δ'_0 have the same meaning as in equation 6 and Fig. 4. Point A represents 1 unit and is the basic unforced diffusion-only situation of equations 1 and 2. Region B, which extends to a normalised mixing layer growth of 50 units, is the situation predicted in various papers, using equations similar to 3 and 4 and which does not factor-in the compressibility issues discussed in section 3. It is *very* dubious whether this is achievable in practice for the reasons already outlined (in other words, region B is probably nonexistent). Region C is the situation portrayed in regions A and B, but assuming that fuel is accelerated as discussed in sections 4 and 5; it extends from 5 units (for diffusive mixing only) to 55 units for good turbulent mixing. Region D, which extends from approximately 10 to 57 units, represents the addition of electrostatic enhancement,

as discussed in section 6, applied to the basic diffusive mixing case of region C – the large range is due to uncertainty in parameters like ion-mobility, which are difficult to measure and not well characterised at high air and fuel temperatures and densities. Finally, region E stretches from approximately 100 to 550 units and assumes electrostatic enhancement, as in region D, and turbulent mixing. The graphs do not include the more speculative mechanisms outlined in section 7. The actual quantitative figures involved can be estimated from equations 1 to 4, the graph in figure 4 coupled with equations 5 and 6 and the information in Tables 1 and 2.

Figure 17b shows how mixing-layer growth decreases with increasing freestream Mach number; the figures are normalised to the situation at Mach 5 and based on Billig’s aerodynamic figures. The decrease in mixing is mainly due to assuming a fixed mixing (longitudinal) length in the engine, but also on other changing parameters like density and increasing temperature. The gray region represents the uncertainty in the figures.

As well as the engine topology discussed earlier in the paper (for example as illustrated in Figs. 8, 10 and 15), other configurations are also possible. The benefits of some of these are discussed in the literature [2, 5]. Figure 18 illustrates two possibilities – diagram *a* shows an “inside out” configuration with the main airflow travelling centrally, and *b* an “interlaced” (sometimes called manifold [2]) configuration. The advantage of the first type is that it may prove less resistant to airflow; it might also be an easier way to produce a combined cycle (air-breathing at lower speeds, rocket-cycle at higher), than the other topologies. In the case of the second type, the purpose is to aid mixing by forcing more contact area between the fuel and the air.

There are many other design variants based on these themes – for example by allowing fuel injection from the centre (spike) of the engine or using Busemann topologies to reduce wave drag. In all these topologies, great care must be taken to engineer the aerodynamics of the duct so that shock-waves produced by the edges of the engine components do not interfere with the mixing process.

There may also be advantages to combining the interlaced configuration with the “pusher” topology discussed in section 5, and using the rotary valve to pulse *both* the air and fuel

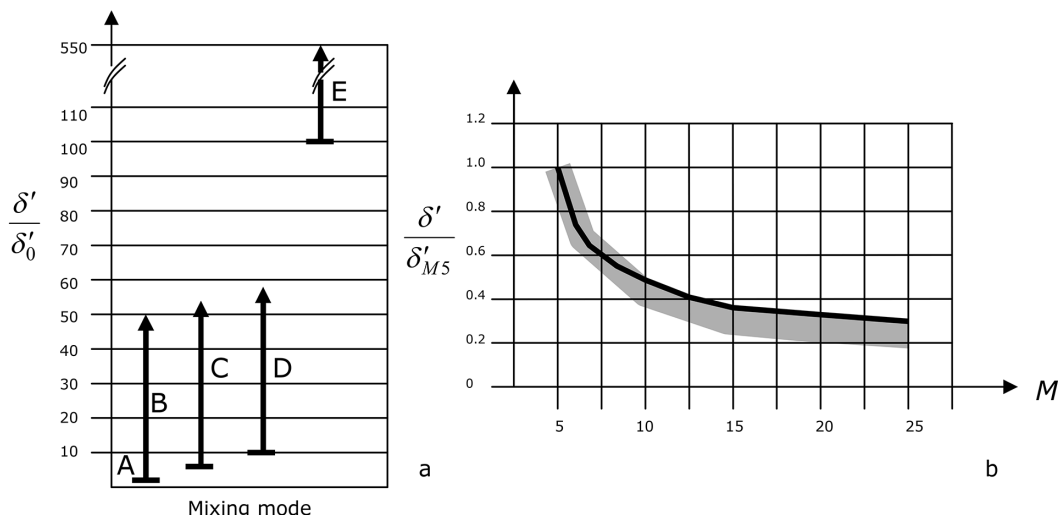


Fig. 17 Predictions of mixing performance based on the previously discussed models.

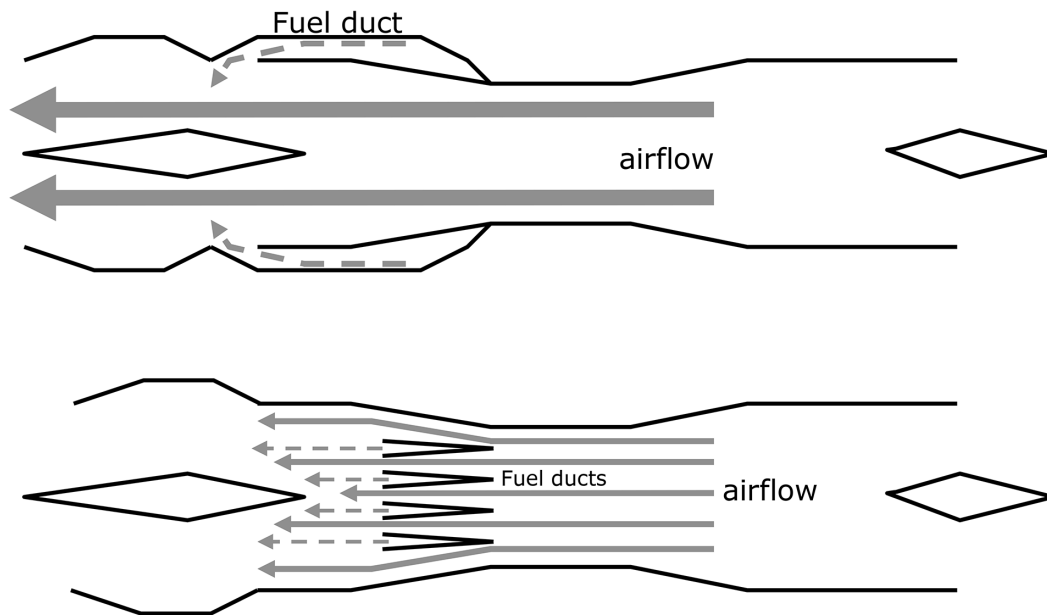


Fig. 18 Alternative engine topologies.

supply. This would produce a true sandwich of both species as shown in Fig. 19, without the edge effects caused by a pulsed fuel component penetrating a continuous air-stream.

If the fuel were premixed with a radiation absorbing gas, as mentioned in section 4, EMA could also be applied, in this case, after injection of the pushed fuel [3].

9. CONCLUSIONS

The main aims of this paper are threefold. Firstly, to discuss the role of compressibility in mixing, provide a literature survey of some of the key papers in the area and illustrate why current engine designs do not live up to expectations. Secondly, to demonstrate that, although simple mixing regimes will probably not be able to provide the required performance, innovative forced mixing methods may be able to. Finally, to provide a variety of potential techniques that might lead to useful mixing enhancement and therefore a working system. The arguments presented in the sections above suggest that the potential improvement in mixing layer growth, using such techniques, is between 5 times (being conservative) and 550 times (being extremely optimistic), over simple injection. The most likely scenario is an improvement of between 10 and 100.

The methods outlined here are not the only ones which might be used to achieve enhanced mixing (for example, the injection and bursting of pressurised fuel capsules in the

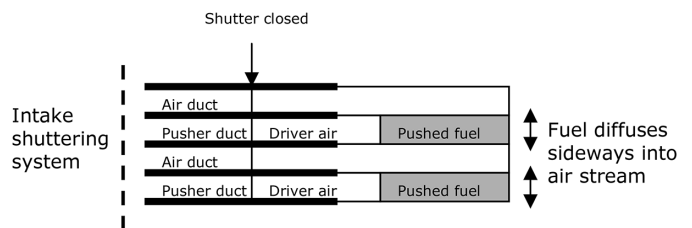


Fig. 19 Pulsing both air and (pushed) fuel.

air-stream has not been discussed, but is another potentially interesting technique, as are innovative heat-exchangers, like those proposed in the SABRE engine [39]). Rather than provide a complete solution, they are meant to stimulate debate on the benefits of forced mixing and also of adapting a multimodal approach to the problem – that is, using several different but complementary methods to achieve a good mixture. Such an approach might be considered rather inelegant, but is probably necessary to overcome the considerable obstacles outlined in the first sections of the paper.

As discussed several times in the preceding sections, it should be remembered that many of the predictions described are subject of large uncertainties. Therefore, the next stage is to try and simulate some of the principles outlined using Computational Fluid Dynamics or similar methods and provide more accurate predictions of performance. However as outlined above, the different principles and forces at play and also the effects of compressibility make this a challenging task.

REFERENCES

1. J.P. Drummond, G.S. Diskin and A.D. Cutler, "Fuel-Air Mixing and Combustion in SCRAMJETs", 38th AIAA/ASME/SAE/ASEE Joint Propulsion Conference, Indianapolis, Indiana, 7-10 July 2002. Paper AIAA-2002-3878.
2. W.H Heiser et al, "Hypersonic Airbreathing Propulsion", AIAA Education Series, Washington, 1994.
3. C. MacLeod, "Electromagnetically Activated Hypersonic Ducts", JBIS, 62, pp.99-109, 2009.
4. C. MacLeod, K.S. Gow and N.F. Capanni, "Some Practical Aspects of Electromagnetic Activation", JBIS, 62, pp.320-331, 2009.
5. E.T. Curran and S.N.B. Murthy, "Scramjet Propulsion", in Progress in Astronautics and Aeronautics, Series, Vol. 189, AIAA, Washington, 2001.
6. F.S. Billig, "Design and development of single stage to orbit vehicles", John-Hopkins Applied Physics Laboratory Technical Digest, 11, pp.336-352, 1990.
7. J.D Anderson, "Fundamentals of aerodynamics (3rd ed)", McGraw-Hill, New York, 2001, pp.538-542.
8. R.B. Bird, W.E. Stewart and E.N. Lightfoot, "Transport Phenomena", Wiley, New York, pp 518-525, 2002.
9. Anon (Compressed Gas Association), "Handbook of Compressed Gases (4th ed)", Kluwer Academic Publishers, Norwell, pp 60-62, 1999.

10. H. Schlichting, "Boundary Layer Theory", McGraw-Hill, New York, 1979.
11. S.N.B. Murthy and E.T. Curran, "High Speed Flight Propulsion Systems", AIAA Progress in Astronautics and Aeronautics Series, **Vol. 137**, AIAA, Washington, 1991.
12. D. Papamoschou and A. Roshko, "The compressible turbulent shear layer: an experimental study," *Journal of Fluid Mechanics*, **197**, pp.453-477, 1988.
13. M.A. Azim and A. K. M. S. Islam, "Turbulent mixing layer from two nonparallel streams", *The Aeronautical Journal*, **107**, pp.241-248, 2003.
14. S.L. Birch and J.M. Eggers, "A critical review of the experimental data for developed free turbulent shear layers", NASA document SP-321, pp.943-949, 1973.
15. G.L. Brown and A. Roshko, "On density effects and large structures in turbulent mixing layers", *Journal of Fluid Mechanics*, **64**, pp.775-781, 1974.
16. J.F. Douglas, J.M. Gasiorek, J.A. Swaffield, "Fluid Mechanics (4th ed)", Pearson (Prentice-Hall), Harlow, 2001, pp.7-9.
17. M.D. Slessor, M. Zhuang and P.E. Dimotakis, "Turbulent shear-layer mixing: growth-rate compressibility scaling", *Journal of Fluid Mechanics*, **414**, pp.35-45, 2000.
18. J.L. Hall, P.E. Dimotakis and H. Rosemann, "Experiments in nonreacting compressible shear layers", *AIAA Journal*, **31**, pp.2247-2254, 1993.
19. T.M. Sugden and C.N. Kenney, "Microwave Spectroscopy of Gases", Van Nostrand, London, 1965.
20. W. Gordy, W.V. Smith and R.F. Trambarulo, "Microwave Spectroscopy", Wiley, New York, 1953.
21. B.H. Stuart, "Infrared Spectroscopy: Fundamentals and applications", Wiley-Blackwell, London, 2004.
22. S. Thorwirth *et al*, "Rotational Spectra of small PAHs", *The Astrophysical Journal*, **662**, pp.1309-1314, 2007.
23. S. Satori *et al*, "The development of a microwave engine", 27th International Electric Propulsion Conference, Pasadena, California, 15-19 October 2001. Paper IEPC-01-224.
24. J.H. Van Vleck, "The absorption of microwaves by uncondensed water vapour", *Physical review*, **71**, pp.425-433, 1947.
25. M. Martinez-Sanchez and J.E. Pollard, "Spacecraft electric propulsion – an overview", *Journal of Propulsion and Power*, **14**, pp.688-699, 1998.
26. J.K. Wright, "Shock tubes (Methuen's Monographs on Physical Subjects)", Spottiswoode Ballantyne and Co, London, 1961.
27. R.V. Vasil'eva *et al*, "Turbulent mixing of driver and driven gases in a shock tube channel", *Journal of applied mechanics and technical physics*, **26**, pp.271-277, 1985.
28. D.J. Griffiths, "Introduction to electrodynamics", Pearson, New Jersey, 1998.
29. H.A. Erickson, "The mobility of argon and hydrogen ions in air", *Physical Review*, **26**, pp.465-468, 1925.
30. H.A. Erickson, "The mobility of acetylene ions in air", *Physical Review*, **28**, pp.372-373, 1926.
31. H. Tammet, "Reduction of air ion mobility to standard conditions", *Journal of Geophysical Research*, **103**, pp.13933-13937, 1998.
32. V.A. Mohnen, "Formation, nature and mobility of ions of atmospheric importance", in *Electrical Processes in Atmospheres*, eds. Dolezalek and Reiter, Steinkopff-Verlag, Darmstadt, 1977, pp.1-17.
33. C. MacLeod, N.F. Capanni, K.S. Gow, "Fuel Encapsulation for Inertial Electrostatic Confinement Nuclear Fusion Reactors", *JBIS*, **64**, pp.139-149, 2011.
34. J.D. Anderson, "Gas Dynamic Lasers: An introduction", Academic Press, New York, 1976.
35. J. Hogan, "Why bombers choose explosives that fall apart", *New Scientist*, **2484**, p.14, 2005.
36. F. Dubnikova *et al*, "Decomposition of Triacetone Triperoxide Is an Entropic Explosion", *Journal of the American Chemical Society*, **127**, pp.1146-1159, 2005.
37. D.W. Bogdanoff, "Advanced Injection and Mixing Techniques for Scramjet Combustors", *Journal of Propulsion and Power*, **10**, pp.183-190, 1994.
38. J.M. Seiner, S.M. Dash and D.C. Kenzakowski, "Historical Survey of Enhanced Mixing in SCRAMJET Engines", *Journal of Propulsion and Power*, **17**, pp.1273-1286, 2001.
39. J.J. Murray, C.M. Hemsell and A. Bond, "An Experimental Pre-cooler for Air-breathing Rocket Engines", *JBIS*, **54**, pp.199-209, 2001.

(Received 26 June 2013; Revision 5 June 2013; Accepted 21 June 2013)

* * *